Stopped-Flow Kinetic Analysis Using Hadamard Transform Time-of-Flight Mass Spectrometry

ARTICLE *in* ANALYTICAL CHEMISTRY · OCTOBER 2010

Impact Factor: 5.64 · DOI: 10.1021/ac101899n · Source: PubMed

4 AUTHORS, INCLUDING:

Richard Zare
Stanford University
1,146 PUBLICATIONS **43,397** CITATIONS

SEE PROFILE

Anal. Chem. **2010,** *82,* 8650–8657

Stopped-Flow Kinetic Analysis Using Hadamard Transform Time-of-Flight Mass Spectrometry

Matthew D. Robbins, Oh Kyu Yoon,† Griffin K. Barbula, and Richard N. Zare*

Department of Chemistry, Stanford University, Stanford, California 94305-5080

A home-built stopped-flow apparatus is interfaced to a Hadamard transform time-of-flight mass spectrometer, which permits study of reaction kinetics with a time between reaction initiation and observation as short as about 100 ms and a sampling rate of chemical change that can approach 1 ms. This technique is applied to the trypsin-catalyzed hydrolysis of several peptides and is validated by comparing the results with literature values as well as to optical data obtained with the present stopped-flow apparatus. In addition, we report a kinetic study of the action of trypsin on a peptide having more than one cleavage site.

Most kinetic assays take advantage of optical labels to detect a chemical conversion or change in the structure of a reactant. In contrast, mass spectrometers can be used as online detectors for chemical or structural changes without optical labels because they measure an intrinsic property: mass-to-charge ratio, m/z. Thus, as long as a reaction results in a change in the mass-to-charge ratio of one reagent, or in the case of reactions resulting in structural isomerism, its fragmentation pattern, the product should be detectable using mass spectrometry. In addition to enabling the use of substrates without chemical labels, a mass spectrometer has the advantage of allowing independent and simultaneous analysis of multiple species, both reactants and products.

Early mass-spectrometry-based biochemical kinetics is comprehensively summarized in a review by Northrop and Simpson,[1] including fast atom bombardment (FAB) mass spectrometry (MS) to study the tryptic hydrolysis[2] and direct sampling from a thermostated reaction vessel into a mass spectrometer for the study of enzymatic reactions.[3] Over the past 10 years there has been an explosion in publications related to the kinetics of enzyme catalysis using mass spectrometry approaches.[4−6] The most common approach to recording kinetics in mass spectrometry involves methods where reactions are quenched and then analyzed. In this scheme aliquots are extracted from an ongoing chemical reaction and then quenched and prepared for electrospray ionization (ESI) or matrix-assisted laser desorption and ionization (MALDI) analysis.

Pulse−chase analysis has also been applied to mass spectrometry. In a pioneering study, Talkington, Siuzdak, and Williamson[7] studied the assembly landscape of the 30S ribosomal subunit with pulse−chase analysis coupled to MALDI mass spectrometry where the pulse was composed of ^{15}N-containing proteins that were extracted from bacteria cultured in isotopically enriched media and the chase contained the ^{14}N equivalent species. The pulse−chase strategy, however, does not allow the study of fast reactions.

To study early time points of rapid reactions or reaction intermediates that are not stable in a chemical quench step, rapid mixing techniques (stopped-flow or continuous-flow methods) must be used. Several groups have developed online, continuous-flow assays for mass spectrometry using a number of strategies. In the most straightforward approach, Konermann, Collings, and Douglas[8] built an ESI-MS continuous-flow apparatus where the distance to the observation point is varied by controlling the length of the capillary between the mixer and the ESI emitter. Using another approach, variation in the observation time point has been controlled by adjusting the reaction volume created in a concentric capillary mixer by Wilson and Konermann[9] where the mixing position and reaction volume are controlled with a stepper motor and can be scanned electronically. Using the Wilson apparatus, reaction time points below 100 ms were analyzed for the first time with an online method using mass spectrometry. In an alternative strategy, Attwood and Geeves[10] have developed continuous-flow systems that function by adjusting the flow rate through a fixed reaction volume. The Attwood and Geeves method allows time points as early as 640 ms to be measured. This technique depends, in part, on the limited variation of the ESI signal in response to changes in the solution flow rate. The Wilson adjustable volume strategy has also been implemented on a microfluidic chip by Rob and Wilson.[11] The application of this method to microfluidic technology holds the promise of simple coupling to the wide variety of lab-on-chip methods that are currently being developed worldwide. One particular drawback to the use of these continuous-flow methods, however, is that a mathematical correction must

* Corresponding author. Phone: (650) 723-3062. Fax: (650) 723-5650. E-mail: zare@Stanford.edu.

† Present address: Department of Molecular and Cell Biology, University of California, Berkeley, CA 94720.

(1) Northrop, D. B.; Simpson, F. B. *Bioorg. Med. Chem.* **1997**, *5*, 641–644.
(2) Smith, L. A.; Caprioli, R. M. *Biomed. Mass Spectrom.* **1984**, *11*, 392–395.
(3) Lee, E. D.; Mueck, W.; Henion, J. D.; Covey, T. R. *J. Am. Chem. Soc.* **1989**, *111*, 4600–4604.
(4) Fabris, D. *Mass Spectrom. Rev.* **2005**, *24*, 30–54.
(5) Kelleher, N. L.; Hicks, L. M. *Curr. Opin. Chem. Biol.* **2005**, *9*, 424–430.
(6) Greis, K. D. *Mass Spectrom. Rev.* **2007**, *26*, 324–339.
(7) Talkington, M. W. T.; Siuzdak, G.; Williamson, J. R. *Nature* **2005**, *438*, 628–632.
(8) Konermann, L.; Collings, B. A.; Douglas, D. *J. Biochem.* **1997**, *36*, 5554–5559.
(9) Wilson, D. J.; Konermann, L. *Anal. Chem.* **2003**, *75*, 6408–6414.
(10) Attwood, P. V.; Geeves, M. A. *Anal. Biochem.* **2004**, *334*, 382–389.
(11) Rob, T.; Wilson, D. J. *J. Am. Soc. Mass Spectrom.* **2009**, *20*, 124–130.

10.1021/ac101899n
Published on Web 09/15/2010

be made to account for the effects of the laminar flow profile.[12] This correction is less important for longer reaction times but can impact the results of data collected for the analysis of early reaction time points, where the continuous-flow approach is most useful and is perhaps the only suitable analytical technique.[13]

Less work has been done on the development of stopped-flow techniques for mass spectrometry. One group, Kolakowski and co-workers,[14,15] has modified a commercial optical stopped-flow system, coupled it with a quadrupole mass spectrometer and an ESI source, and used it to study acid-induced chlorophyll demetalation, the alkaline hydrolysis of acetylcholine, and the denaturation of myoglobin. In another approach, Ørsnes, Graf, and Degn[16] have shown that a rotating ball inlet, similar in design to a ballpoint pen, where a sapphire ball is connected to a volume undergoing a reaction, can be used to introduce mixed solutions through the evaporation of a thin film of solution into a mass spectrometer with an electron impact ionization source to study the reactions of small molecules on the time scale of 100 ms. Using their rotating ball inlet device, Ørsnes and co-workers were able to study the reactions of acetone and butanone with S(IV) species. The Ørsnes method provides a stopped-flow option that is appropriate for the analysis of small, volatile molecules, a limited class of reactants and products. One disadvantage to the modification of a commercial stopped-flow system, as in the Kolakowski case, is the added expense and complexity of the modified equipment. A preferable method would be to construct a dedicated stopped-flow device that was not engineered for the expense and complexity of an optical measurement. The construction of such a device is detailed in this work.

The mass spectrometer coupled to a stopped-flow device should provide high spectral rates of several hundred spectra per second. This requirement led us to use Hadamard transform time-of flight mass spectrometry (HT-TOFMS), a form of time-of-flight mass spectrometry based on ion beam modulation−demodulation. In past work it was shown that the HT-TOFMS apparatus can record individual mass spectra at a rate approaching 2500 per second.[17] In traditional time-of-flight mass spectrometry (TOFMS), individual ion packets are introduced into a drift region and the flight times of ions are measured. In HT-TOFMS, however, instead of introducing individual pulses of ions into a field-free region, we spatially modulate a continuous ion beam between two discrete states at megahertz rates according to a pseudorandom sequence. This spatial modulation takes the form of deflection of the ion beam off the axis of its initial propagation using a specialized device called a Bradbury−Nielsen gate (BNG).[18−20] The Bradbury−Nielsen gate is designed to allow short deflection rise times and to confine the physical region within which the ions experience deflection. A delay-line imaging detector measures the position and flight time of every ion arrival at the detector from both states of ion beam deflection, and thus, HT-TOFMS has a 100% duty cycle for continuous ion sources such as electrospray. The theory of HT-TOFMS is well developed and is described in detail elsewhere.[17,21]

The key requirement of a kinetic experiment is to record as a function of time a signal's value with high precision and subsequently convert it into concentration information. In mass spectrometry the measured value is a peak height or area. The measure of relative height or peak area stability is the peak height precision, the ratio of the peak height to its own standard deviation. HT-TOFMS has a peak height precision (PHP) advantage over traditional, on-axis TOFMS given by

$$\frac{\mathrm{PHP}_i^{\mathrm{HT}}}{\mathrm{PHP}_i^{\mathrm{conv}}} = \sqrt{\frac{f^{\mathrm{HT}}}{f^{\mathrm{conv}}} F_i}$$

Here, $\mathrm{PHP}_i^{\mathrm{HT}}$ and $\mathrm{PHP}_i^{\mathrm{conv}}$ are the PHPs of analyte i in 100% duty cycle Hadamard and conventional TOF modes, f is the duty cycle, and F_i is the fractional abundance of ion i. This equation can be used to consider the suitability of an HT-TOFMS experiment in place of any other MS measurement whose duty cycle is known. As long as the fractional abundance of the ion species exceeds the duty cycle ratio, HT-TOFMS will provide a PHP advantage in any measurement. This PHP advantage is maximized for detection schemes that require evaluation over a larger mass-to-charge window. Data acquisition over a larger mass-to-charge window gives MS-based kinetic analysis the capability to monitor the evolution of more complex reactions. The PHP enhancement is most pronounced for spectra collected on shorter time scales with less signal averaging, which constitutes a distinct advantage in kinetic studies. In these cases the inherent PHP, a function of the number of ions counted, is lower. Thus, HT-TOFMS potentially provides an ideal experimental tool for the mass spectrometric analysis of chemical reactions.

We report on a new stopped-flow system constructed using a mixer and a rapid-switching multiway, two-state valve that employs the HT-TOFMS apparatus as a detector. The stopped-flow apparatus was used to study the trypsin-catalyzed hydrolysis of polypeptides. In the present realization, reactions are studied over the course of minutes, although the technique has intrinsically much faster data acquisition times. The data collected using HT-TOFMS are validated on a chromophoric polypeptide amide model system before being applied to a pair of nonchromophoric polypeptides. To show the capacity for monitoring simultaneous or sequential reactions, the results of the hydrolysis of a polypeptide with two tryptic cleavage sites are explored.

EXPERIMENTAL SECTION

Stopped-Flow Kinetic Apparatus. A stopped-flow kinetic apparatus that uses HT-TOFMS as a detector was constructed from commercially available components (Figure 1). The device contains syringes, mixers, a pump, and a two-state valve. Two syringes, S1 and S2, are rapidly driven by a high-pressure syringe

(12) Wilson, D. J.; Konermann, L. *Anal. Chem.* **2004**, *76*, 2537–2543.
(13) Konermann, L. *J. Phys. Chem. A* **1999**, *103*, 7210–7216.
(14) Kolakowski, B. M.; Konermann, L. *Anal. Biochem.* **2001**, *292*, 107–114.
(15) Kolakowski, B. M.; Simmons, D. A.; Konermann, L. *Rapid Commun. Mass Spectrom.* **2000**, *14*, 772–776.
(16) Orsnes, H.; Graf, T.; Degn, H. *Anal. Chem.* **1998**, *70*, 4751–4754.
(17) Kimmel, J. R.; Yoon, O. K.; Zuleta, I. A.; Trapp, O.; Zare, R. N. *J. Am. Soc. Mass Spectrom.* **2005**, *16*, 1117–1130.
(18) Yoon, O. K.; Zuleta, I. A.; Robbins, M. D.; Barbula, G. K.; Zare, R. N. *J. Am. Soc. Mass Spectrom.* **2007**, *18*, 1901–1908.
(19) Zuleta, I. A.; Barbula, G. K.; Robbins, M. D.; Yoon, O. K.; Zare, R. N. *Anal. Chem.* **2007**, *79*, 9160–9165.
(20) Bradbury, N. E.; Nielsen, R. A. *Phys. Rev.* **1936**, *49*, 388.
(21) Yoon, O. K.; Zuleta, I. A.; Kimmel, J. R.; Robbins, M. D.; Zare, R. N. *J. Am. Soc. Mass Spectrom.* **2005**, *16*, 1888–1901.

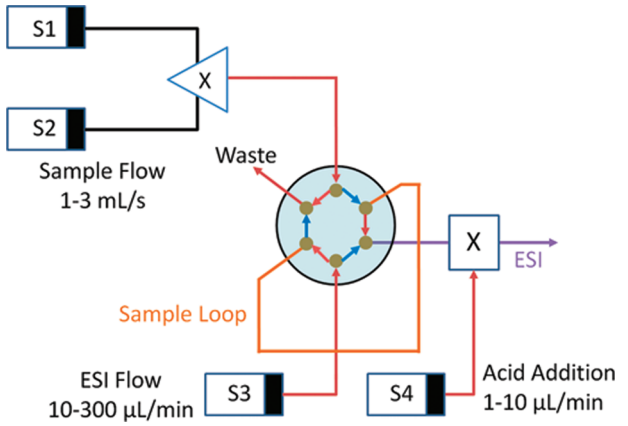

Figure 1. Schematic diagram of the stopped-flow apparatus. The valve configuration using blue or red arrows demonstrates the load phase or the inject phase of operation, respectively. Mixers are labeled by X and liquid sources by S. See the text for a full description.

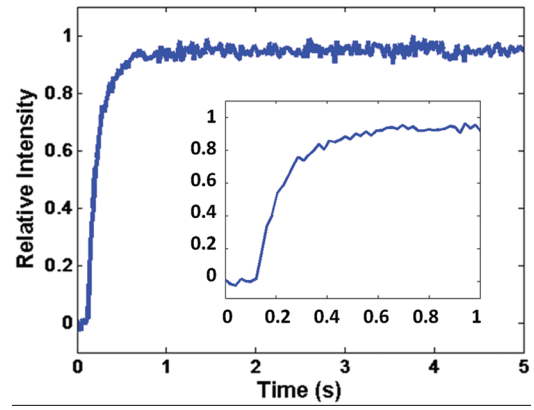

Figure 2. Experimental determination of the dead time. The inset figure shows the early time points.

Table 1. Mathematical Estimate of the Dead Time in the Stopped-Flow Apparatus Calculated from the Device's Swept Volume[a]

fill step	fill time (ms)	cumulative total (ms)
mixer	11.5	11.5
to valve	23.0	34.5
sample loop	27.4	61.9
valve switch	5.0	66.9
valve exit	63.8	130.7
ESI emitter	70.6	201.3

[a] For this table a value of >2 mL/s for the sample filling flow rate and an ESI delivery rate of 100 µL/s were used.

pump (PhD 2000, Harvard Apparatus, Holliston, MA) to produce a total flow rate of 1−3 mL/s. The flow from the two syringes is combined in X1 using a Berger−Ball mixer (Olis Inc., Bogart, GA), and the output fills a sample loop (orange in Figure 1) on a multiway, two-state valve[22] during the load phase of the valve (blue arrows in Figure 1). The two-state valve has an 80 PSI helium-driven pneumatic actuator (C2H-200A, VICI Valco, Inc., Houston, TX), controlled using an accessory (HSSI, VICI Valco), and can switch between the states in less than 10 ms.[23] While the sample loop is filled, stable nebulization-assisted electrospray is maintained by the continuous flow of a tracer solution in the same solvent as the reacting species. The tracer solution contains at least one compound that can be monitored by mass spectrometry during the period before and after a stopped-flow kinetic measurement. The liquid flow for ESI is provided by an HPLC pump (AD-10, Shimadzu Scientific Instruments, Columbia, MD), indicated as S3 in Figure 1. The HPLC pump provides a more stable flow rate than a syringe pump used in the same configuration. Additionally, the HPLC pump can provide the higher backing pressure necessary for high flow rate ESI through a narrow ESI emitter. The inject phase (red arrows in Figure 1) begins by the triggering of the pneumatic actuator, which switches the state of the two-state valve. In this phase, the ESI flow is directed so that the reacting solution in the sample loop is pushed to the ESI emitter through mixer X2, which adds a small volume of acidic solution, pumped by S4, to aid the electrospray process. The switching of the two-state valve results in the output of a TTL pulse that is transformed into an NIM pulse with a 10 µs delay using a delay generator (100C Pulse Generator, Systron Donner, Concord, CA). The time of the NIM pulse is recorded using the time-to-digital convertor for the delay-line anode detector. During analysis of kinetic data, the time of this switch trigger pulse is used as the primary reference time.

In this design the maximum observation time is limited by the volume of the sample loop, the minimum swept volume, and the rate of analyte flow to the ESI emitter. The sample observation time, the amount of time needed to deplete the contents of the sample loop, is coupled to the point of earliest analysis, which is reduced by using a higher ESI flow rate.

The dead time, the time between mixing the two reagents and the first reaction data point collected by the mass spectrometer, is dominated by the analyte travel time from the mixer to the ESI emitter. In the stopped-flow configuration, a 50 µL sample loop and the associated flow path can be filled in approximately 60 ms using the syringe pump. The sample loop and all tubing are constructed from 0.030 in. poly(ether ether ketone) (PEEK). The use of the large 0.030 in. fluidic components is necessitated by the maximum possible backing pressure of the syringe pump. The use of smaller diameter tubing would reduce the dead time. The two-state valve has been modified to reduce its contribution to the dead time of the experiment and minimize its swept volume during the inject state. While most of the through-holes in the stator are 0.030 in. and match the diameter of the PEEK sample loop, the through-hole for the ESI emitter port has been reduced to 0.010 in. This reduction in diameter addressed the largest contribution to the dead time. Because the ESI emitter port is never directly connected to the output of the mixer, this reduction in diameter is not controlled by the pressure limitations of the syringe pump. Using this system, a total dead time of approximately 200 ms can be achieved by using a high ESI flow rate to direct the output of the valve into the mass spectrometer. The rise time of an analyte signal as measured by the mass spectrometer is shown in Figure 2.

Table 1 provides the contribution of each step in the fluid transfer process from sample mixing to analysis by the mass spectrometer at an ESI flow rate of 100 µL/s. From the table it can be seen that the largest contributions to the dead time occur

(22) Berger, R. L.; Balko, B.; Chapman, H. F. *Rev. Sci. Instrum.* **1968**, *39*, 493–498.
(23) Harvey, M. C.; Robinson, R. E.; Harvey, M. C.; Stearns, S. D. *J. Chromatogr. Sci.* **1994**, *32*, 190–194.

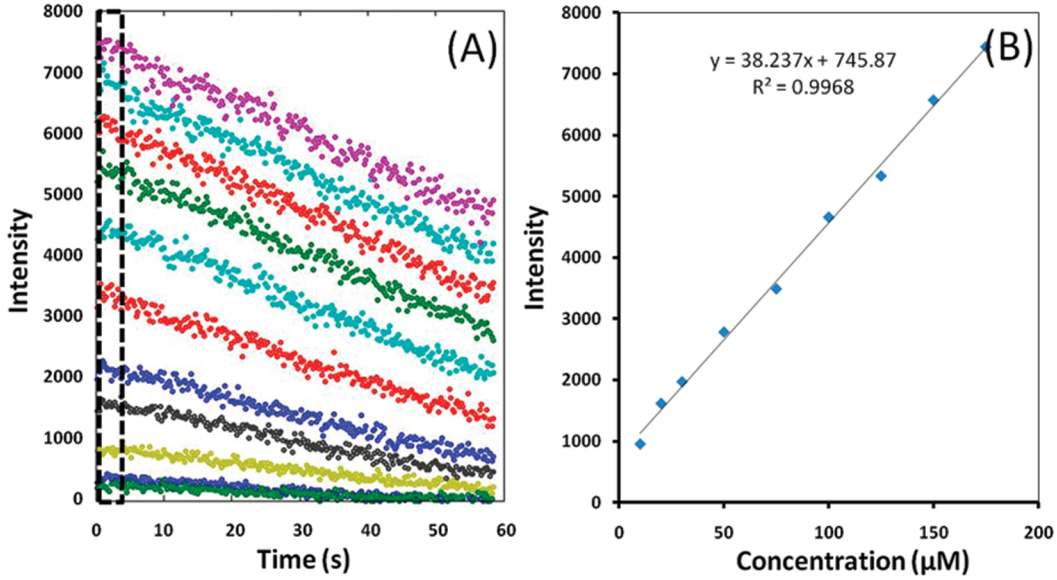

Figure 3. Calibration strategy for kinetic analysis: (A) signal versus time for different concentrations and (B) calibration curve obtained by using the early time points enclosed by the box in (A).

after filling of the sample loop and are the times required to sweep fluid through the 0.010 in. port in the valve and the transit through the ESI emitted capillary. These values can be reduced by narrowing their volumes, using a smaller or shorter ESI capillary, purchasing a valve with a smaller exit port, or increasing the ESI flow rate. Currently, the narrowest size valve port available from VICI in any valve configuration is 0.004 in. in diameter. Reducing this one diameter to the lowest manufactured value would reduce the swept volume of the valve exit by 80%. The effect on the measured dead time would likely exceed the reduction in swept volume. This expected nonlinearity is related to the mixing of the analyte and tracer solutions caused by the diameter mismatch at this stage. As can be seen from Figure 2 and Table 1, the nonflow contributions to the dead time, the extended signal rise time, are as significant as swept-volume effects. By completing the listed modifications, the total dead time for the stopped-flow system could be reduced to less than 100 ms.

Calibration of Kinetic Data. Figure 3 details the calibration strategy for the kinetic work. Early time points, as shown by the box in Figure 3A, which correspond to the consumption of 1−2% of the substrate, are averaged and plotted against the initial concentration of substrate to form the calibration curve, shown in Figure 3B. The calibration curve allows a conversion of intensity values to concentration information. Fits of the calibrated data can then be used to construct a plot of the initial rate of enzymatic hydrolysis versus substrate concentration. The use of these initial values to form a calibration curve simplifies the design of the kinetic experiment by making the calibration procedure internal to the mass spectrometric analysis. For this reason, we did not pursue fitting the appearance of the products.

Simulation of Enzymatic Progress Curves. For the trypsin-catalyzed hydrolysis of peptide with two cleavage sites, we generated simulated time traces or progress curves from the Michaelis−Menten rate equations using k_{cat} and K_M values as parameters to be optimized. Starting from the experimental concentrations at 120 s and using a time step of 0.1 s, the concentrations of the substrate, intermediates, and products at each time point were computed from the calculated concentrations at the previous time step. This procedure was repeated from 120 to 520 s. Errors between the simulated and experimental progress curves were calculated by summing the squares of the differences between the two concentrations. The k_{cat} and K_M values that minimized the error between the simulated and experimental progress curves were chosen.

Hadamard Transform Time-Of-Flight Mass Spectrometer. The instrumentation has been described in detail elsewhere.[24] Briefly, the HT-TOFMS instrument is a reflectron ESI-TOFMS apparatus with 100% duty cycle based on ion beam modulation and ion imaging. The ion source is salvaged from a Mariner TOFMS (PerSeptive Biosystems, Framingham, MA) system. Custom-built rf and dc power supplies were used to control the ion source.[25] Other components include a BNG beam modulation system[18,26] and an imaging detector composed of a multichannel plate stack with a delay line anode (DLD80, RoentDek Handels GmbH, Kelkheim-Ruppertshain, Germany).[27]

Chemicals. Peptide samples were acquired from various vendors. *N*-Benzoyl-L-phenylalanyl-L-valyl-L-arginine-4-nitroanaline (BPVApNA), a chromophoric artificial trypsin substrate, was obtained from Sigma-Aldrich (St. Louis, MO). VGVRVR was obtained from American Peptide (Sunnyvale, CA). The samples of VGVKVR and VGVRVGVKVGVH were purchased from GenScript USA (Piscataway, NJ). Water (W2-4) and triethylammonium bicarbonate buffer (pH 8.5) were also purchased from Sigma-Aldrich.

The trypsin sample was reductively methylated and treated with TPCK by the manufacturer to reduce chymotryptic and

(24) Yoon, O. K.; Robbins, M. D.; Zuleta, I. A.; Barbula, G. K.; Zare, R. N. *Anal. Chem.* **2008**, *80*, 8299–8307.
(25) Robbins, M. D.; Yoon, O. K.; Zuleta, I.; Barbula, G. K.; Zare, R. N. *Rev. Sci. Instrum.* **2008**, *79*, 034702−034707.
(26) Bolton, C. *Electron. Des. News* **2002**, 88.
(27) Jagutzki, O.; Mergel, V.; Ullmann-Pfleger, K.; Spielberger, L.; Spillmann, U.; Dörner, R.; Schmidt-Böcking, H. *Nucl. Instrum. Methods Phys. Res., Sect. A* **2002**, *477*, 244–249.

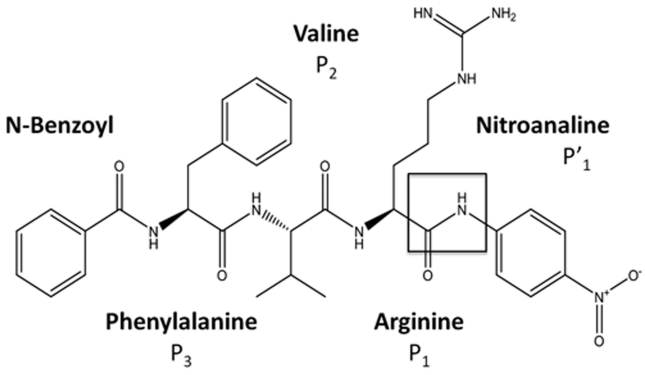

Figure 4. Structure of BPVApNA with a square box surrounding the hydrolysis site.

autolytic activity.[28] Reductive methylation stabilizes trypsin toward autolysis by passivating active lysine residues that have some surface exposure and has been shown not to interfere with the enzyme's catalytic activity.[29] TPCK, L-(1-tosylamido-2-phenyl) chloromethyl ketone, is a permanent, selective inhibitor for the enzyme chymotrypsin that does not have an effect on the action of trypsin.[30] The trypsin sample chosen is from the variety commonly used in proteomics experiments for mass spectrometry. The trypsin sample was used from 20 μg ampules at the stated weight and corrected to a standard activity in *N*-benzoyl-L-arginine ethyl ester (BAEE) units using the lot analysis provided.

Both the enzyme and peptide samples were dissolved in 2 mM triethylammonium bicarbonate buffer. The peptide sample stock solutions were titrated with additional sodium hydroxide solution to bring their pH to within 0.1 unit of pH 8.5.

RESULTS AND DISCUSSION

The stopped-flow system was first tested on the tryptic hydrolysis of the chromophoric substrate BPVApNA (Figure 4). The 4-nitroaniline leaving group of BPVApNA absorbs in the blue when it is free in solution and does not absorb in the visible region of the optical spectrum when in its amide form. The N-terminal of the peptide has been capped with an *N*-benzoyl group so that the charge at the amine does not interfere with enzyme action. In Figure 4 we use the Schechter and Berger notation[31] for protease−substrate interaction where the amino acid residues are labeled counting in both directions from the scissile bond as P_1, P_2, and P_3 on the amino-terminal side and P_1', P_2', and P_3' on the carboxy-terminal side. BPVApNA is part of a class of chromophoric artificial amide and ester substrates whose tryptic digests have been studied in detail. This family of substrates includes BAEE and *N*-benzoyl-L-arginine-*p*-nitroanaline (BAPNA), among others.[32,33]

The absorbance of 4-nitroaniline (pNA) at a series of concentrations was determined by allowing the BPAVpNA solution to react completely with trypsin over a 6 h period. After this reaction delay period, solution absorbance was measured on a Cary 6000i (Varian Cary, Palo Alto, CA) spectrophotometer, and these absorbance values were used to construct a calibration curve. An OLIS RSM-1000 (Online Instrument Systems, Inc., Bogart, GA) equipped with a Stopped-Flow USA (Online Instrument Systems) was used for the optical kinetic measurements, and the results are shown in Figure 5A. The experiment was also performed using the stopped-flow apparatus and the HT-TOFMS detector, and the results are shown in Figure 5B. The optical stopped-flow data were collected under the same temperature (22.5 ± 1 °C) and solution conditions as the mass spectrometry data.

Parts A and B of Figure 5 show that both the UV−vis and MS stopped-flow methods are in reasonable agreement with each other. Table 2 lists the Michaelis−Menten parameters calculated by fitting the initial rate data (dashed curves in Figure 5). The error bars in Figure 5A,B represent the standard deviation of triplicate measurements. Both measured values are similar to the literature reported values for the Michaelis−Menten parameters.[34]

After verification of the stopped-flow MS apparatus with BPVApNA, the device was applied to the study of the hydrolysis of two unlabeled polypeptides by trypsin. The peptides VGVRVR and VGVKVR were selected to allow comparison of the kinetic parameters for two polypeptides that vary only in their trypsin-active residue, K (arginine) and R (lysine), rather than in combination with adjacent residues. Additionally, these particular sequences were selected because trypsin prefers an amino acid sequence with an aliphatic species in the P_1' site and hydrolyzes them at a faster rate than other moieties in that position.[35] Different enzyme concentrations (100/200 nM) were used for the two different samples so that significant consumption of the substrate occurred over the course of the observation time window.

Parts C and D of Figure 5 show the resulting Michaelis−Menten plots for the hydrolysis of the peptides VGVRVR and VGVKVR. Both plots are fit well by Michaelis−Menten kinetics; all of the points match the fit within error, where the error bars have the same meaning as in Figure 5A,B. Neither plot exhibits inhibition of enzyme action at the highest concentrations studied. Table 2 summarizes the results of the experiments and compares them to published data on related chromophoric systems.[36] There has been no independent study that shows how much the chromophoric label alters the kinetics. Nevertheless, the general trends across systems are conserved, with larger values for k_{cat} and smaller values for K_m for the arginine-containing polypeptide versus its lysine-containing analogue. Thus, on examining all the data in Table 2, we conclude that the present approach is capable of providing accurate Michaelis−Menten parameters for a number of trypsin-catalyzed hydrolyses.

To demonstrate further the capabilities of the present stopped-flow MS system, we studied the trypsin-catalyzed hydrolysis of a polypeptide, VGVRVGVKVGVH, with two cleavage sites. This peptide was designed to contain both R and K cleavage sites and to preserve the near-cleavage motifs in the P_1−P_3 and the P_1'

(28) Sigma-Aldrich. *Product Information*; Saint Louis, MO, 2002.
(29) Rice, R. H.; Means, G. E.; Brown, W. D. *Biochim. Biophys. Acta, Protein Struct.* **1977**, *492*, 316–321.
(30) Carpenter, F. H. *Methods Enzymol.* **1967**, *11*, 237–237.
(31) Schechter, I.; Berger, A. *Biochem. Biophys. Res. Commun.* **1967**, *27*, 157–162.
(32) Schwert, G.; Takenake, Y. *Biochim. Biophys. Acta* **1955**, *16*, 570–575.
(33) Erlanger, B. F.; Kokowsky, N.; Cohen, W. *Arch. Biochem. Biophys.* **1961**, *95*, 271–278.
(34) Lottenberg, R.; Christensen, U.; Jackson, C. M.; Coleman, P. L. *Methods Enzymol.* **1981**, *80*, 341–361.
(35) Kurth, T.; Grahn, S.; Thormann, M.; Ullmann, D.; Hofmann, H.-J.; Jakubke, H.-D.; Hedstrom, L. *Biochemistry* **1998**, *37*, 11434–11440.
(36) Grahn, S.; Ullmann, D.; Jakubke, H.-D. *Anal. Biochem.* **1998**, *265*, 225–231.

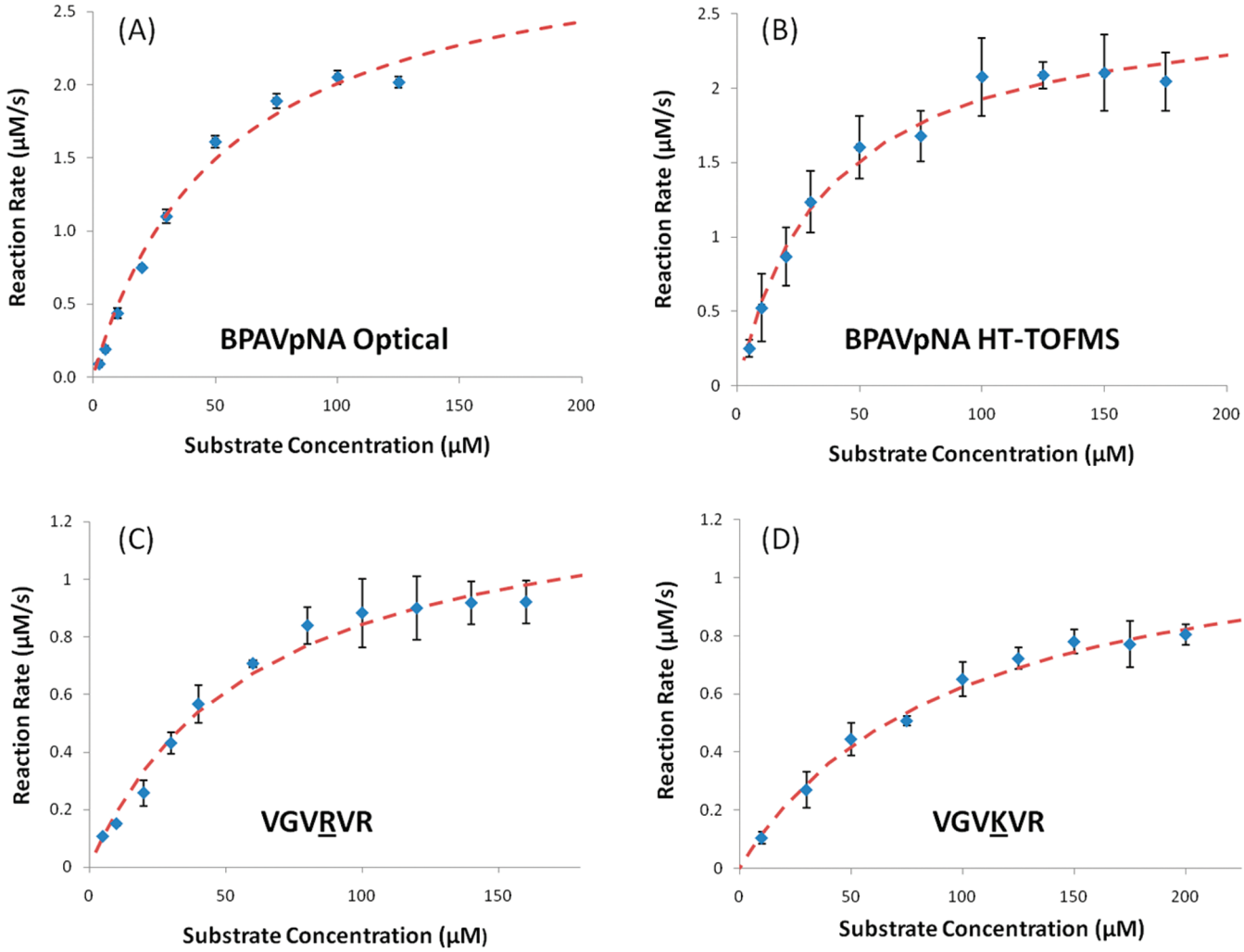

Figure 5. Initial reaction rates as a function of the substrate concentration for the tryptic hydrolysis of BPVApNA, VGVRVR, and VGVKVR using UV−vis detection in (A) and HT-TOFMS in (B)−(D). The dashed curve in each plot is the result of a fit to the Michaelis−Menten equation. The error bars are described in the text.

sites of the previously studied VGVXVR polypeptides. As shown in Figure 6A, this new polypeptide can be hydrolyzed through two pathways based upon the first residue hydrolyzed to form three common products, VGVR, VGVK, and VGVH. Table 3 shows the m/z ratio for each species. Each of the products and intermediate fragments contains a basic residue on the C-terminal fragment to improve sensitivity of that species to mass spectral analysis using ESI in the positive mode.

Enzymatic reactions having multiple pathways do not lend themselves to the method of initial rates used for the VGVXVR system. Instead, we analyzed the time traces of substrates, intermediates, and products at a single initial substrate concentration of approximately 400 μM. The experimental conditions for the analysis of VGVRVGVKVGVH were similar to those used for the studies of VGVRVR and VGVKVR. The reaction was performed in 2 mM triethylammonium bicarbonate buffer at 22.5 ± 1 °C against 100 nM trypsin (final concentration). However, to accommodate a longer observation period, the volume of the sample loop was increased to 200 μL and the ESI flow rate was reduced to 15 μL/min. A corresponding reduction in the quantity of acetic acid added to the solution at the second mixer was also made. These alterations were made at the expense of an increased

Table 2. Comparison of the Michaelis−Menton Parameters[a] for the Steady-State Hydrolysis Kinetics of Amide Substrate Species by Trypsin Using Stopped-Flow UV−Vis Spectrophotometry, Stopped-Flow Fluorescence (F), or Stopped-Flow HT-TOFMS (MS)

substrate	k_{cat} (s^{-1})	K_m (μM)	k_{cat}/K_m ($s^{-1}\cdot\mu M^{-1}$)
BPVApNA (UV−vis)[34]	28 ± 1.4	38 ± 4	0.74 ± 0.08
BPVApNA (UV−vis)	32 ± 2.4	53 ± 9	0.60 ± 0.1
BPVApNA (MS)	27 + 1.2	36 ± 5	0.75 ± 0.1
VGVRVR (MS)	15 ± 1	60 ± 10	0.25 ± 0.04
VGVKVR (MS)	6.4 ± 0.4	93 ± 13	0.07 ± 0.01
DABCYL-GPARLAIG-EDANS (F)[36]	40 ± 2.5	34 ± 3	1.17 ± 0.2
DABCYL-GPAKLAIG-EDANS (F)[36]	10 ± 1	58 ± 5	0.176 ± 0.02
Tos-GPR-AMC (UV−vis)[36]	94 ± 2	14 ± 1	1.3 ± 0.3
Tos-GPK-AMC (UV−vis)[36]	49 ± 0.1	37 ± 2	6.5 ± 0.3

[a] The Michaelis−Menten parameters are defined in the traditional manner for the process

$$E + S \underset{k_{-1}}{\overset{k_1}{\rightleftarrows}} ES \xrightarrow{k_2} E + P$$

where $k_{cat} = k_2$ and $K_M = (k_{-1} + k_2)/k_1$.

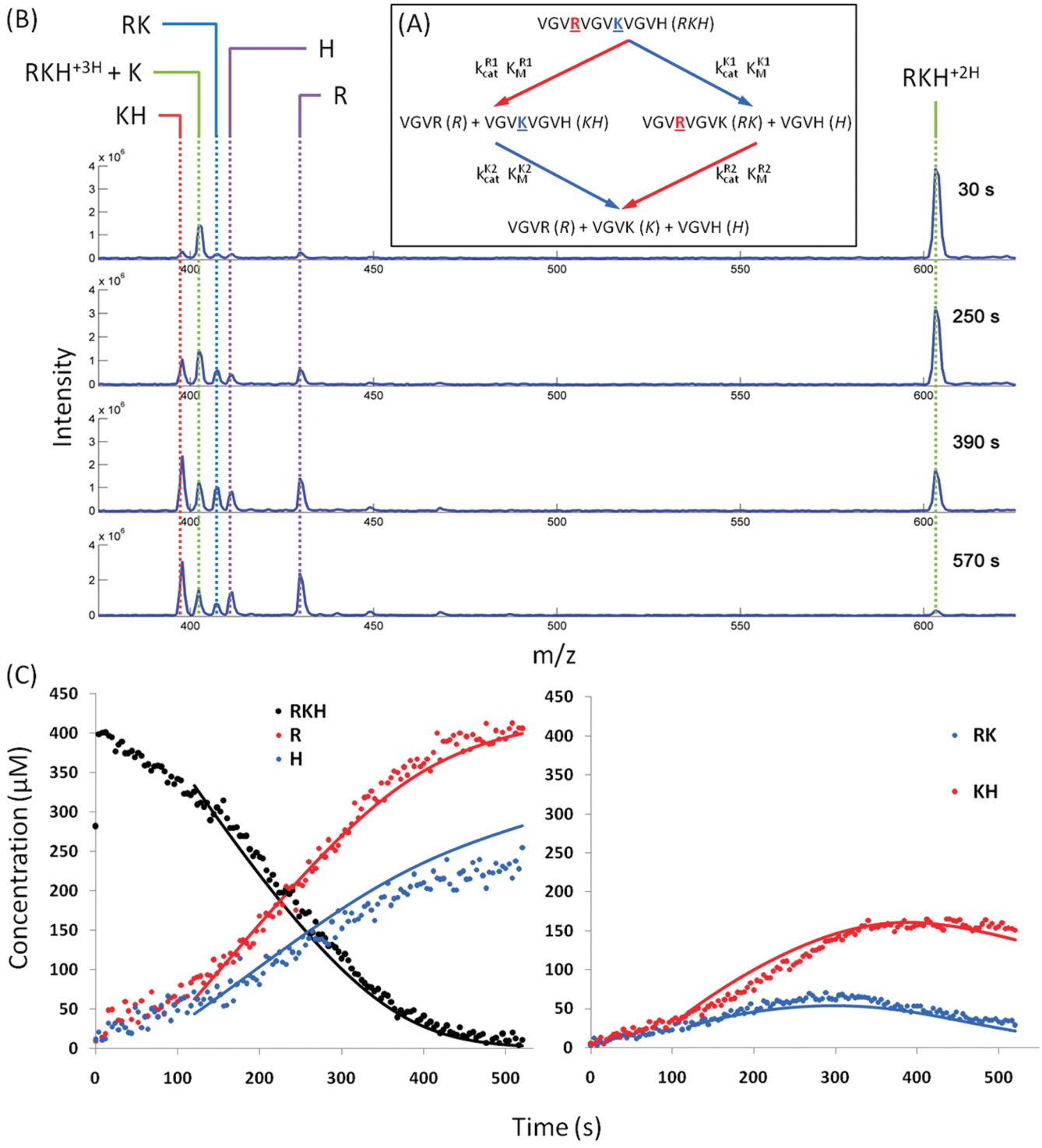

Figure 6. Tryptic hydrolysis of VGVRVGVKVGVH: (A) two degradation pathways; (B) mass spectra at four time points; (C) concentration versus time for various species indicated. Both experimental measurements (dots) and simulations (solid lines) are shown.

observation dead time of 2 s, which is a less important parameter for systems that require longer observation windows.

Figure 6B shows the mass spectra at four time points during an entire 9 min kinetic run analyzing the hydrolysis of VGVRVGVKVGVH by trypsin. The spectrum shows the expected peaks detailed in Table 3. The species of eight amino acid residues or longer all appear predominately in their +2 charge state, while the tetrapeptide reaction products all appear at +1 species. Unfortunately, the +3 charge state from VGVRVGVKVGVH overlaps with the +1 charge state for VGVK at the experimental resolution, and independent time traces for each species cannot be generated.

Figure 6C shows the extracted reaction progress curves for the largest peaks of principal products of the VGVRVGVKVGVH hydrolysis scheme detailed in Figure 6A. The initial substrate concentration of VGVRVGVKVGVH is well above the K_m values measured for the VGVXVR systems, and all of the initial substrate is consumed over the 9 min reaction time. To extract

Table 3. Mass-to-Charge Values for All Species in the Reaction Network for the Hydrolysis of the 12-Residue Peptide VGVRVGVKVGVH Shown in Figure 6[a]

species	m/z (Da)
VGVRVGVKVGVH (+1)	1206
VGVRVGVK (+1)	813.5
VGVKVGVH (+1)	794.5
VGVRVGVKVGVH (+2)	603.5
VGVR	430.3
VGVH	411.2
VGVRVGVK (+2)	407.3
VGVRVGVKVGVH (+3)	402.6
VGVK	402.2
VGVKVGVH (+2)	397.8

[a] Residues that are cut by trypsin are underlined.

Michaelis−Menten parameters from the progress curves, we constructed simulated progress curves assuming steady-state Michaelis−Menten kinetics, where the reaction rates are

$$\frac{d[RKH]}{dt} = -\frac{E_0 k_{cat}^{R1}[RKH]}{K_M^{R1} + [RKH]} - \frac{E_0 k_{cat}^{K1}[RKH]}{K_M^{K1} + [RKH]}$$

$$\frac{d[KH]}{dt} = \frac{E_0 k_{cat}^{R1}[RKH]}{K_M^{R1} + [RKH]} - \frac{E_0 k_{cat}^{K2}[KH]}{K_M^{K2} + [KH]}$$

$$\frac{d[RK]}{dt} = -\frac{E_0 k_{cat}^{R2}[RK]}{K_M^{R2} + [RK]} + \frac{E_0 k_{cat}^{K1}[RKH]}{K_M^{K1} + [RKH]}$$

$$\frac{d[R]}{dt} = \frac{E_0 k_{cat}^{R1}[RKH]}{K_M^{R1} + [RKH]} + \frac{E_0 k_{cat}^{R2}[RK]}{K_M^{R2} + [RK]}$$

$$\frac{d[K]}{dt} = \frac{E_0 k_{cat}^{R2}[RK]}{K_M^{R2} + [RK]} + \frac{E_0 k_{cat}^{K2}[KH]}{K_M^{K2} + [KH]}$$

$$\frac{d[H]}{dt} = \frac{E_0 k_{cat}^{K1}[RKH]}{K_M^{K1} + [RKH]} + \frac{E_0 k_{cat}^{K2}[KH]}{K_M^{K2} + [KH]}$$

Here, E_0 is the initial enzyme concentration. Progress curves of enzymatic reactions containing multiple pathways are difficult to solve using integrated Michaelis−Menten equations.[37] Thus, we generated simulated progress curves using four different k_{cat} and K_M values as parameters until the error between the experimental and simulated progress curves was minimized as explained in the Experimental Section. The best fit curves are shown as solid lines in Figure 6C, and the parameters are

$$k_{cat}^{R1} = 12\ s^{-1} \qquad K_M^{R1} = 90\ \mu M$$

$$k_{cat}^{K1} = 7\ s^{-1} \qquad K_M^{K1} = 90\ \mu M$$

$$k_{cat}^{R2} = 10\ s^{-1} \qquad K_M^{R2} = 90\ \mu M$$

$$k_{cat}^{K2} = 5\ s^{-1} \qquad K_M^{K2} = 90\ \mu M$$

As defined in Figure 6A, the rate of the R1 process proceeds faster than the K1 process, in keeping with the observation from the VGVXVR experiments where the arginine residue was more active toward hydrolysis by trypsin than the lysine residue. This behavior is seen in the raw spectra of Figure 6B, where the VGVKVGVH (+2) peak becomes the dominant feature in the spectrum at long times. Similarly, the R2 arginine hydrolysis process is faster than the corresponding K2 lysine hydrolysis process. This phenomenon is seen in the second panel of Figure 6C where the KH (+2) signal, the reaction product from the R1 process, levels out while the RK (+2) signal, the intermediate stage in the K1−R2 sequence, falls at longer reaction times. Thus, the time course of the reaction kinetics is clearly revealed by stopped-flow HT-TOFMS.

CONCLUSIONS

This work shows the potential advantages to using stopped-flow HT-TOFMS for the analysis of chemical and biochemical reaction kinetics. The experimental method was validated by comparing the optical and mass spectrometric stopped-flow analyses of a chromophoric artificial trypsin substrate. Two new, native polypeptide samples were studied, for which no kinetic values for trypsin hydrolysis were available in the literature. In a final experiment, the hydrolysis of a polypeptide with two potential hydrolysis sites, arginine and lysine, was evaluated to demonstrate the capability of this method to monitor multiple species in a reaction. The present study represents a proof of principle for interfacing stopped-flow methodology with HT-TOFMS. The technique appears to have the capability of following reaction kinetics with reasonable precision that take place on the order of minutes, and future work might be directed to much more rapid reaction processes.

ACKNOWLEDGMENT

This work was supported by the Air Force Office of Scientific Research under Grant FA 9550-10-1-0235.

NOTE ADDED AFTER ASAP PUBLICATION

This paper was published on September 15, 2010, with an error in the equation in the footnote of Table 2. The corrected version was reposted on September 20, 2010.

Received for review July 16, 2010. Accepted August 26, 2010.

AC101899N

(37) Duggleby, R. G.; Daniel, L. P. *Methods Enzymol.* **1995**, *249*, 61–90.